Theory of laser-molecule interaction: The recursive-residue-generation method

André Nauts* and Robert E. Wyatt
Department of Chemistry, The University of Texas, Austin, Texas 78712
(Received 27 December 1983)

General properties of the semiclassical time propagator are given for molecules in interaction with intense laser fields, i.e., for molecular systems advanced by a periodic time-dependent operator. The operator expression of Floquet's theorem is used to unify various approaches in the literature and to emphasize that the problem can be reduced to a time-independent one with an effective quasienergy operator, if evolution is only considered at multiples of the optical period. The Magnus expansion (through third order) is used to obtain an explicit expression for the quasienergy operator. The recursive-residue-generation method, devised to evaluate transition amplitudes for systems with a very large number of coupled states, is developed in detail and applied to the model problem (with over 3×10^3 states) of an anharmonic oscillator, dipole coupled to the laser and also linearly coupled to a multimode harmonic bath.

I. INTRODUCTION

Over the past few years, the theory of excitation of atoms and molecules by intense lasers has advanced considerably.[1] Nonperturbative calculations within the dressed state or the semiclassical molecule-field descriptions, in addition to those employing the rotating-wave and other approximations, have been performed on a number of small molecules or for relatively small subsets of states in larger molecules. These calculations were restricted to fewer than one thousand states, since eigenvectors of large matrices were required. In order to bypass this bottleneck, in this study a new approach to the multistate problem is formulated and applied to a model; calculations with many more than 10^3 states are possible.

We will begin the formulation within the semiclassical theory; the molecule is regarded as a *quantum* system and the radiation as an externally provided *classical* periodic field. This problem is then equivalent to the general problem of a quantum system advanced by a periodic *time-dependent* Hamiltonian. Such systems are effectively studied by means of Floquet theory.[2–12] In Sec. II A, we first review how the operator formulation of Floquet theory[10–12] leads to a factorization of the time propagator into periodic and exponential aperiodic components. This leads to the significant result that the time-dependent system can be advanced by means of a *time-independent* effective Hamiltonian M, the quasienergy operator, provided that time intervals are discretized by observing the system only at integer multiples of the optical cycle. Moreover, the operator expression of Floquets theorem is systematically used to unify various approaches relating to Floquet theory. Then, in Secs. II B and II C, we show how the propagator can be more fully specified by the additional assumptions of symmetry and reality of the periodic Hamiltonian. In particular, a discrete microreversibility principle can be derived, similar to the usual microreversibility principle, but only valid for multiples of the optical period. Finally, in Sec. II D, the Magnus expansion of the time-propagator[8,13] is used, along with results from the preceding section, to obtain an explicit expression (through third order) for the effective time-independent Hamiltonian.

In Sec. III, we detail the new recursive residue generation method[14] (RRGM) which is particularly adept at calculating, in complete generality, transition amplitudes, $\langle f \mid \exp(-iMt \mid \hbar) \mid i \rangle$, between two arbitrary states, $\mid i \rangle$ and $\mid f \rangle$, and where M is any time-independent Hamiltonian. In this method, which focuses on transition amplitudes one at a time, the key feature is the recursive generation of residues of the Green operator associated with the propagator $\exp(-iMt \mid \hbar)$, thus avoiding the necessity of calculating eigenvectors of large matrices. The residues are generated by employing the Lanczos method[15–20] to recursively convert the Hamiltonian matrix to tridiagonal form—a structure which greatly facilitates the calculation of eigenvalues. The residues are then calculated directly from several sets of eigenvalues of tridiagonal matrices.

Development of the RRGM was particularly inspired by studies of the Cambridge solid-state physics group[21–23] on the electronic structure of disordered solids. Their emphasis was on computation of the local density of electronic states about a site in the disordered solid. In other applications, Lanczos recursion and Lanczos polynomials have been used in several areas, including studies of the Jahn-Teller effect,[24] spacings of molecular vibrational eigenvalues,[25] magnetic resonance line shapes,[26] and photoionization.[27] In particular, since the time-dependent interaction of molecules with intense lasers can be reduced to a time-independent problem by using an effective Hamiltonian to advance the system, Sec. IV is devoted to numerical study of a model consisting of an anharmonic oscillator, dipole coupled to the laser and linearly coupled to a multimode harmonic bath. Emphasis is placed upon characteristics of residue spectra, with comparisons between results from matrix diagonalization and the RRGM. A summary of the method is presented in Sec. V.

II. FLOQUET THEORY

The linear, unitary time propagator, $U(t \mid t_0)$, is evolved by the time-dependent Schrödinger equation

$$\begin{aligned} &H(t)U(t \mid t_0)=i\hbar\frac{dU(t \mid t_0)}{dt} , \\ &H(t)=H_0+H_1(t) , \\ &U(t_0 \mid t_0)=1 . \end{aligned} \tag{1}$$

In the present section, which was inspired by earlier work in Ref. 8(c), we will see how the expression for the time propagator is restricted by assuming several properties for the Hamiltonian operator. Section II A is mainly devoted to the operator expression of Floquet's theorem,[10–12] which results from assuming periodicity of the Hamiltonian in time, and to its relation to other formalisms used in the literature. In Sec. II B, we derive a property of the propagator resulting from assuming reality and time symmetry of the Hamiltonian about a given instant, whereas in Sec. II C we go through the consequences of combining the assumptions of Secs. II A and II B, i.e., that a "discrete microreversibility principle" can be obtained together with the reality of the quasienergy operator introduced in Floquet's theorem. Finally, in Sec. II D an explicit expression for that operator is given in the case of sinusoidal time dependence.

A. Properties resulting from the periodicity of the Hamiltonian in time

When the Hamiltonian is periodic in time, $H_1(t+\tau)=H_1(t)$, then the propagator has the following properties.

(1) For evolution through n cycles (n is an integer)

$$U(t_0+n\tau \mid t_0)=[U(t_0+\tau \mid t_0)]^n . \tag{2}$$

This relation can be easily proven from Eq. (1) (see also Refs. 10 and 12).

(2) The evolution operator may be factored into a unitary time-dependent periodic operator times the exponential of a "unitless" Hermitian *time-independent* operator:

$$\begin{aligned} &U(t \mid t_0)=P(t \mid t_0)e^{-i\omega \mathrm{M}(t-t_0)} , \\ &P(t+\tau \mid t_0)=P(t \mid t_0), \quad P(t_0 \mid t_0)=1 . \end{aligned} \tag{3}$$

This is an expression, in operator language, of the well-known Floquet theorem.[9–12]

Now, let us write the eigenvalue equation for the *quasienergy operator* $M=\hbar\omega \mathrm{M}$, where $\hbar\omega$ is the photon energy,

$$M \mid \alpha\rangle = \mid \alpha\rangle\epsilon_a . \tag{4}$$

These (real-valued) eigenvalues and eigenvectors will be called *quasienergies* (or Floquet energies) and *Floquet states,* respectively. Spectral properties of the operator M have been discussed by Gesztesy and Mitter.[11] Next, multiplying the Schrödinger equation (1) on the right by the Floquet state $\mid \alpha\rangle$ and replacing $U(t \mid t_0)$ by its expansion, Eq. (3), we obtain

$$\left[H(t)P(t \mid t_0)-i\hbar\frac{dP(t \mid t_0)}{dt}\right] \mid \alpha\rangle = P(t \mid t_0) \mid \alpha\rangle\epsilon_\alpha . \tag{5}$$

The time-dependent vectors $P(t \mid t_0) \mid \alpha\rangle$ are called *steady states* whose r representation is the $u(r,t)$ of Sambe.[9]

The relation to the matrix formalism used by Wyatt and co-workers[8] is easily seen: First, denote the field-free eigenstates by $\{ \mid k\rangle \}$,

$$H_0 \mid k\rangle = \mid k\rangle E_k^0 . \tag{6}$$

By using the closure relation

$$\sum_\alpha \mid \alpha\rangle\langle\alpha \mid = 1 \tag{7}$$

the transition amplitude between the (field-free) states $\mid i\rangle$ and $\mid f\rangle$, i.e., the (f,i) matrix element of Eq. (3) becomes

$$\langle f \mid U(t \mid t_0) \mid i\rangle = \sum_\alpha \langle f \mid P(t \mid t_0) \mid \alpha\rangle \times e^{-i\epsilon_\alpha(t-t_0)/\hbar}\langle\alpha \mid i\rangle . \tag{8}$$

Then, if we put

$$\begin{aligned} &\langle f \mid U(t \mid t_0) \mid i\rangle = U_{fi}(t \mid t_0) , \\ &\langle f \mid P(t \mid t_0) \mid \alpha\rangle = \Phi_{f\alpha}(t) , \\ &\langle\alpha \mid i\rangle = \langle\alpha \mid P^{-1}(t_0 \mid t_0) \mid i\rangle = \Phi^*_{\alpha i}(t_0) , \\ &\frac{\epsilon_\alpha}{\hbar} = \mu_\alpha\omega , \end{aligned} \tag{9}$$

Eq. (8) for the $i \rightarrow f$ transition amplitude becomes

$$U_{fi}(t \mid t_0)=\sum_\alpha \Phi_{f\alpha}(t)e^{-i\mu_\alpha\omega(t-t_0)}\Phi^*_{\alpha i}(t_0) \tag{10}$$

or, in terms of matrices,

$$U(t \mid t_0)=\Phi(t)e^{-i\mu\omega(t-t_0)}\Phi^{-1}(t_0) . \tag{11}$$

Moreover, the relation with Shirley's time-independent matrix formalism[2] may be seen as follows: since $P(t \mid t_0)$ is a periodic operator, it may be Fourier expanded

$$P(t \mid t_0)=\sum_{m=0,\pm1,\ldots} e^{im\omega(t-t_0)}D^m(t_0) . \tag{12}$$

Multiplying on the right by $\mid \alpha\rangle$, and using the closure relation for the molecular states $\{ \mid k\rangle \}$, then gives

$$P(t \mid t_0) \mid \alpha\rangle = \sum_k \sum_m \mid k,m\rangle D^{(\alpha)}_{km} , \tag{13}$$

where

$$\mid k,m\rangle = \mid k\rangle e^{im\omega(t-t_0)}$$

may be regarded as *dressed molecular states,* and $D^{(\alpha)}_{km}=\langle k \mid D^m \mid \alpha\rangle$ are the coefficients for the expression of a steady state in the dressed molecular basis. Next, from Eq. (4), with

$$H_1(t)=\tfrac{1}{2}\mu E^0(e^{i\omega t}+e^{-i\omega t}) ,$$

first using the closure relation for the dressed molecular states

$$\sum_{k,m} |k,m\rangle\langle k,m| = 1 , \tag{14}$$

and then multiplying on the left by $\langle k',m'|$, we obtain

$$\sum_m \sum_k [(E_k^0 + m\hbar\omega)\delta_{k'k}\delta_{m'm} + V_{k'k}(\delta_{m',m+1}+\delta_{m',m-1})]D_{km}^{(\alpha)} = \epsilon_\alpha D_{k'm'}^{(\alpha)} ,$$

where

$$V_{k'k} = \tfrac{1}{2}E^0\langle k'|\mu|k\rangle .$$

This equation is identical to the one derived by Shirley.[2]

B. Property resulting from the reality and symmetry of the Hamiltonian about a time t_0^*

If we assume that there exits a time t_0^* about which the Hamiltonian is symmetric, i.e.,

$$KH(t_0^*+t)K = H(t_0^*-t) \tag{15}$$

and that the Hamiltonian is real

$$KH(t_0^*+t)K = H(t_0^*+t) , \tag{16}$$

where K is the antiunitary complex conjugation operator with the properties[28(a)]

$$K = K^\dagger , \quad K^2 = 1 , \tag{17}$$

then, the unitary time propagator has the following property:

$$U(t_0^*+t\,|\,t_0^*) = KU(t_0^*-t\,|\,t_0^*)K \tag{18}$$

for all times t. Indeed, $U(t_0^*+t\,|\,t_0^*)$ is determined by the Schrödinger equation

$$H(t_0^*+t)U(t_0^*+t\,|\,t_0^*) = i\hbar\frac{dU(t_0^*+t\,|\,t_0^*)}{dt} . \tag{19}$$

If we change t into $-t$ and take the complex conjugate of both sides of Eq. (19), we obtain, in view of Eqs. (15), (16), and (17)

$$H(t_0^*+t)(KU(t_0^*-t\,|\,t_0^*)K) = i\hbar\frac{d(KU(t_0^*-t\,|\,t_0^*)K)}{dt} . \tag{20}$$

Thus we see that

$$U(t_0^*+t\,|\,t_0^*)$$

and

$$KU(t_0^*-t\,|\,t_0^*)K$$

are solutions of the same differential equation and since they have the same initial conditions, i.e.,

$$U(t_0^*\,|\,t_0^*) = KU(t_0^*\,|\,t_0^*)K = 1 ,$$

they are equal.

C. Property resulting from the periodicity, the reality and the symmetry of the Hamiltonian

Let us assume that the Hamiltonian is periodic (of period τ), in addition to being real and symmetric about t_0^*, and let us take $t = n\tau$ with $n = \pm1, \pm2, \ldots$. By Floquet's theorem [Eqs. (3) and (4)] we know that

$$U(t_0^* \pm n\tau\,|\,t_0^*) = \exp\left[\mp\frac{i}{\hbar}M(n\tau)\right] , \tag{21}$$

where M is the Hermitian time-independent quasienergy operator. Inserting Eq (21) into Eq. (18), we obtain

$$\exp\left[-\frac{i}{\hbar}M(n\tau)\right] = K\exp\left[+\frac{i}{\hbar}M(n\tau)\right]K$$

or still

$$\exp\left[-\frac{i}{\hbar}M(n\tau)\right] = \exp\left[-\frac{i}{\hbar}(KMK)(n\tau)\right] . \tag{22}$$

Hence the quasienergy operator is real,

$$M = KMK \tag{23}$$

which entails that the Floquet states $|\alpha\rangle$ may always be taken as real, thus reducing by half the recursion calculations (see Sec. III B).

The quasienergy operator being Hermitian, time independent and real, we also have the obvious relation

$$\exp\left[-\frac{i}{\hbar}M(n\tau)\right] = K\left[\exp\left[-\frac{i}{\hbar}M(n\tau)\right]\right]^\dagger K \tag{24}$$

or still (for any initial time t_0)

$$U(t_0+n\tau\,|\,t_0) = KU^\dagger(t_0+n\tau\,|\,t_0)K \tag{25}$$

which may be regarded as the expression of a *discrete microreversibility principle.* Indeed Eq. (25) resembles the usual expression of the microreversibility principle [see for instance Ref. 28(b)] but is distinct from it in that it only holds for the discrete times $t_0+n\tau$ ($n = 0, \pm1, \ldots$). This brings out once again that a physical problem with a periodic Hamiltonian reduces to a time-independent problem with an effective quasienergy operator if the evolution is only considered at times $t_0+n\tau$.

D. Magnus expansion of the quasienergy operator

An explicit expression for the quasienergy operator M can be developed by means of the Magnus expansion[13] (for a different approach, see Ref. 10), where $\Omega_n(t)$ is the nth-order term,

$$\exp\left[-\frac{i}{\hbar}M\tau\right] = \exp\left[-\frac{i}{\hbar}\sum_{n=1}^{\infty}\Omega_n(\tau)\right] , \tag{26}$$

or

$$M\tau = \sum_{n=1}^{\infty}\Omega_n(\tau) , \tag{27}$$

where, for example, through second order,

$$\Omega_1(\tau)=\int_{t_0}^{t_0+\tau} H(t_1)dt_1 \ , \tag{28a}$$

$$\Omega_2(\tau)=\frac{i}{2\hbar}\int_{t_0}^{t_0+\tau} dt_2 \int_{t_0}^{t_2} dt_1[H(t_1),H(t_2)] \ . \tag{28b}$$

It is a well-known property of the Magnus expansion that the $\Omega_n(\tau)$ are Hermitian operators, which implies that

$$\sum_{n=1}^{\infty} \Omega_n(\tau)$$

is, in its turn, Hermitian, which agrees with the fact that $M\tau$ itself has to be Hermitian.

Moreover, requiring in addition that $M\tau$ should be real [see Eq. (23)], entails

$$\sum_{k \text{ even}} \Omega_k(\tau)=0 \tag{29}$$

since $\Omega_k(\tau)$ (k even) are pure imaginary operators (when the Hamiltonian is real) as can be seen from the general expressions for $\Omega_n(\tau)$, given for instance in Table II of Ref. 8(c).

Thus we are left with the expansion

$$M\tau=\sum_{l \text{ odd}} \Omega_l(\tau) \ . \tag{30}$$

When the time-dependent perturbation is of the form

$$H_1(t)=V_r\cos(\omega t) \tag{31}$$

the explicit expressions for $\Omega_l(\tau)$ ($l=1$ and 3) are (we used the symbolic language MACSYMA to derive these results)

$$\Omega_1(\tau)=H_0\tau \ , \tag{32a}$$

$$\Omega_3(\tau)=-\frac{1}{\hbar^2\omega^2}\{[H^0,[H^0,V_r]]-\tfrac{1}{4}[V_r,[H^0,V_r]]\}\tau \tag{32b}$$

from which we see that

$$M_l=\frac{1}{\tau}\Omega_l(\tau) \quad (l=1 \text{ and } 3) \tag{33}$$

is a time-independent (and of course also real and Hermitian) operator. It therefore seems safe to conjecture that relation (33) holds for all odd values of l. To sum up

$$M=\sum_{l \text{ odd}} M_l \ , \tag{34}$$

where M_l is a *real time-independent Hermitian* operator.

It is clear that any truncation of the summation in Eq. (34) gives rise to an operator having the required properties for M, i.e., to be real, time independent, and Hermitian. In other words, the properties required for the operator M are fulfilled term-wise by the M_l operators.

III. RECURSIVE RESIDUE GENERATION METHOD: RRGM

As seen in the preceding section, it is a consequence of Floquet's theorem, Eq. (3), that evolution through time intervals which are multiples of the optical period τ is governed by the propagator

$$U(t_0+n\tau \mid t_0)=\exp\left[-\frac{i}{\hbar}M(n\tau)\right] \ . \tag{35}$$

As a result, the transition amplitude between field-free molecular eigenstates belonging to the spectrum of H^0 is given by

$$\langle f \mid U(t_0+n\tau \mid t_0) \mid i\rangle=\left\langle f\left|\exp\left[-\frac{i}{\hbar}(H_0+V)(n\tau)\right]\right|i\right\rangle \ , \tag{36}$$

where $V=M-H^0$ may be regarded as the time-independent perturbation inducing transitions when M advances the system to multiples of τ. It should be emphasized here that the method developed below does *not* explicitly rely on M being a quasienergy operator and $n\tau$ being a multiple of the optical period, but can be used for *any* transition amplitude of the type

$$\langle f \mid U(t_0+t \mid t_0) \mid i\rangle=\left\langle f\left|\exp\left[-\frac{i}{\hbar}Mt\right]\right|i\right\rangle \ , \tag{37}$$

i.e., for transition amplitudes between two arbitrary states, $|i\rangle$ and $|f\rangle$, and where M is any time-independent Hamiltonian, which advances the system to any time t. The method, which is based on recursive generation of the residues of Green functions, will be termed the recursive residue generation method (RRGM).[14]

A. Green functions

As is well known (see, e.g., Ref. 29), Eq. (37) may be expressed in terms of the resolvent

$$g(\zeta)=(\zeta\mathbb{1}-M)^{-1} \tag{38}$$

as follows:

$$\langle f \mid U(t_0+t \mid t_0) \mid i\rangle=\frac{1}{2\pi i}\int_C d\zeta\, e^{-i\zeta t}G_{fi}(\zeta) \ , \tag{39}$$

where the contour C runs from $+\infty$ to $-\infty$, parallel to the real axis just above the singularities of the "off-diagonal" Green function

$$G_{fi}(\zeta)=\langle f \mid g(\zeta) \mid i\rangle \ .$$

The starting point of the RRGM is, however, different: using both the eigenvalue equation

$$M \mid \alpha\rangle=\mid \alpha\rangle\epsilon_\alpha \tag{40}$$

and the closure relation

$$\sum_{\alpha=0}^{N-1} \mid \alpha\rangle\langle\alpha \mid =1 \ , \tag{41}$$

the transition amplitude, Eq. (37), may also be expressed as

$$\langle f \mid U(t_0+t \mid t_0) \mid i\rangle=\sum_{\alpha=0}^{N-1} \langle f \mid \alpha\rangle\langle\alpha \mid i\rangle e^{-i\epsilon_\alpha t/\hbar} \ . \tag{42}$$

Direct calculations of the eigenstates $|\alpha\rangle$ being impractical, if not impossible for $N \geq 10^3$, it is important to note, and it is the very gist of the RRGM, that Eq. (42) can be

evaluated *without* directly computing the eigenvectors $|\alpha\rangle$, by using the following ideas.

(i) The coefficient $\langle f|\alpha\rangle\langle\alpha|i\rangle$ can be expressed as a linear combination of, at most, four positive numbers:[30]

$$\langle f|\alpha\rangle\langle\alpha|i\rangle=\tfrac{1}{2}(|\langle u|\alpha\rangle|^2-|\langle v|\alpha\rangle|^2+i|\langle w|\alpha\rangle|^2-i|\langle z|\alpha\rangle|^2), \tag{43}$$

where the four *transition vectors* are

$$\begin{aligned}|u\rangle&=\frac{1}{\sqrt{2}}(|i\rangle+|f\rangle),\\ |v\rangle&=\frac{1}{\sqrt{2}}(|i\rangle-|f\rangle),\\ |w\rangle&=\frac{1}{\sqrt{2}}(|i\rangle+i|f\rangle),\\ |z\rangle&=\frac{1}{\sqrt{2}}(|i\rangle-i|f\rangle).\end{aligned} \tag{44}$$

(ii) Next, let us consider the matrix elements of the resolvent, i.e., the Green functions, with respect to the kets $|A\rangle$ and $|B\rangle$,

$$G_{AB}(\zeta)=\langle A|(\zeta 1-M)^{-1}|B\rangle, \tag{45}$$

where $|A\rangle,|B\rangle=|i\rangle$, $|f\rangle$, $|u\rangle$, $|v\rangle$, $|w\rangle$, or $|z\rangle$. Once again, using the closure relation, Eq. (41), we obtain

$$G_{AB}(\zeta)=\sum_{\alpha=0}^{N-1}\frac{\langle A|\alpha\rangle\langle\alpha|B\rangle}{\zeta-\epsilon_\alpha}, \tag{46}$$

in which $\langle A|\alpha\rangle\langle\alpha|B\rangle$ is recognized as the residue $R_{AB}(\alpha)$ corresponding to the simple pole ϵ_α of the Green function $G_{AB}(\zeta)$. Moreover, since

$$R_{AA}(\alpha)=|\langle\alpha|A\rangle|^2, \tag{47}$$

and since $|A\rangle$ is normalized, the diagonal residues $R_{AA}(\alpha)$ are bounded and add to unity:

$$0\le R_{AA}(\alpha)\le 1, \tag{48a}$$

$$\sum_{\alpha=0}^{N-1}R_{AA}(\alpha)=1 \tag{48b}$$

(Parseval's relation). In terms of the residues, Eq. (43) can now be written

$$R_{fi}(\alpha)=\tfrac{1}{2}[R_{uu}(\alpha)-R_{vv}(\alpha)+iR_{ww}(\alpha)-iR_{zz}(\alpha)] \tag{49}$$

and the $i\to f$ transition amplitude, Eq. (42), becomes

$$\langle f|U(t_0+t|t_0)|i\rangle=\sum_{\alpha=0}^{N-1}R_{fi}(\alpha)e^{-i\epsilon_\alpha t/\hbar}. \tag{50}$$

The transition amplitude is thus an N-term expansion in which the coefficients of the exponentials are given by Eq. (49), i.e., expressed in terms of the residues of *diagonal Green functions,* which can be explicitly constructed [see (iv) below].

(iii) The residue $R_{AB}(\alpha)$ is by its very definition (see, e.g., Ref. 31)

$$R_{AB}(\alpha)=\lim_{\zeta\to\epsilon_\alpha}[(\zeta-\epsilon_\alpha)G_{AB}(\zeta)]. \tag{51}$$

(iv) Focusing upon the explicit construction of the diagonal Green functions $G_{AA}(\zeta)$, let us use an orthonormal basis in which $|A\rangle$ is the *first* member in order to express the matrix M corresponding to the operator M. By the rule to invert matrices we have

$$G_{AA}(\zeta)=\langle A|(\zeta 1-M)^{-1}|A\rangle=\frac{\det[\zeta 1-M]^{(A)}}{\det[\zeta 1-M]}=\frac{\prod_{\alpha=1}^{N-1}(\zeta-\epsilon_\alpha^{(A)})}{\prod_{\alpha=0}^{N-1}(\zeta-\epsilon_\alpha)}, \tag{52}$$

where $[\zeta 1-M]^{(A)}$ is the *reduced matrix* obtained by deleting the first row and column from $[\zeta 1-M]$. The eigenvalues of M and $M^{(A)}$ are $\{\epsilon_\alpha\}$ and $\{\epsilon_\alpha^{(A)}\}$, respectively. From Eqs. (51) and (52), the residue is then the product of $(N-1)$ factors (each typically the order of unity):

$$R_{AA}(\alpha)=\Gamma_{1,0}^{(A)}(\alpha)\Gamma_{2,1}^{(A)}(\alpha)\cdots\Gamma_{\alpha,\alpha-1}^{(A)}(\alpha)\Gamma_{\alpha+1,\alpha+1}^{(A)}(\alpha)\cdots\Gamma_{N-1,N-1}^{(A)}(\alpha), \tag{53}$$

where

$$\Gamma_{\beta,\gamma}^{(A)}(\alpha)=(\epsilon_\alpha-\epsilon_\beta^{(A)})/(\epsilon_\alpha-\epsilon_\gamma). \tag{54}$$

The significant result is that diagonal residues, and hence transition amplitudes [see Eqs. (49) and (50)] can be computed directly from five sets of eigenvalues, $\{\epsilon_\alpha\}$, $\{\epsilon_\alpha^{(u)}\}$, $\{\epsilon_\alpha^{(v)}\}$, $\{\epsilon_\alpha^{(w)}\}$, and $\{\epsilon_\alpha^{(z)}\}$ without explicitly constructing eigenvectors.

For the usual case where $\langle f|\alpha\rangle$ and $\langle\alpha|i\rangle$ are real numbers, i.e., when $|i\rangle$, $|f\rangle$, and M are real (see Sec. II C when M is a quasienergy operator), Eq. (49) reduces to

$$R_{fi}(\alpha)=\tfrac{1}{2}[R_{uu}(\alpha)-R_{vv}(\alpha)] \tag{55}$$

so that only *three* sets of eigenvalues are needed, $\{\epsilon_\alpha\}$, $\{\epsilon_\alpha^{(u)}\}$, and $\{\epsilon_\alpha^{(v)}\}$, thus reducing by half the recursion calculations.

B. Recursive method for tridiagonalization

In order to generate the sets of eigenvalues needed to compute residues in Eq. (53), we will use the Lanczos recursion method[15–20] to convert the quasienergy matrix M into a Jacobi (tridiagonal) matrix J. With the exception of a diagonal matrix, the Jacobi representation of the quasienergy operator is that which is most compact. Once the diagonal $\{a_0,a_1,\ldots\}$ and off-diagonal $\{b_1,b_2,\ldots\}$ elements of J have been computed, the eigenvalues are obtained quickly [in about 10% of the total

CPU (central processing unit) time] and with no additional storage by use of the EISPACK routine TQLRAT. Tridiagonalizing M is best viewed as the result of a transformation from the original molecular basis $\{|k\rangle, k=1,2,\ldots,N\}$ to the *recursion basis* $\{|n\rangle, n=0,1,\ldots,N-1\}$. In effect, we are transforming M with the matrix of recursion vectors U, $U^{\dagger}MU=J$, although the procedure is done in steps, with no need to store the whole transformation matrix U. In this new basis, the only nonzero matrix elements of operator M, i.e., the nonzero elements of matrix J, are the diagonal *self-energies* (a_n) and the nearest-neighbor *coupling energies* (b_n). The result is that we have converted the original problem, with a complex network of interstate couplings, to a *one-dimensional (Hückel type) disordered lattice.* We will refer to a_n and b_{n+1} as specifying *one link in this one-dimensional chain used to portray* J (e.g., see Ref. 32).

In the Lanczos algorithm, as reformulated by Paige,[18] each recursion step *"forges a new link in the chain."* Starting with the initial recursion vector $|0\rangle$, after forming the vector $M|0\rangle$, the first self-energy is $a_0=\langle 0|M|0\rangle$. The residual vector $\{M|0\rangle-|0\rangle a_0\}$ is then formed; its norm determines the first coupling element in J, $b_1=||M|0\rangle-|0\rangle a_0||^{1/2}$. The next normalized recursion vector is then $|1\rangle=(M|0\rangle-|0\rangle a_0)/b_1$. Now, given the recursion vectors $|n\rangle$ and $|n-1\rangle$, and the previous chain link (a_{n-1},b_n) in fast storage, the next chain link is then generated from the explicit three-term recurrence relation

$$|n+1\rangle=\{M|n\rangle-|n\rangle a_n-|n-1\rangle b_n\}/b_{n+1}\,, \tag{56}$$

where $a_n=\langle n|M|n\rangle$, and b_{n+1} normalizes the *residual vector,* $\{M|n\rangle-|n\rangle a_n-|n-1\rangle b_n\}$. By construction, at least in infinite precision arithmetic, each recursion vector is implicitly orthogonal to all previous ones. In order to start the recursion, we choose either $|0\rangle=|u\rangle$ or $|0\rangle=|v\rangle$. A very important feature of this procedure is that only two recursion vectors are needed in fast storage in order to build the next vector.

Having generated the sets of self-energies and off-diagonal coupling energies from the starter $|0\rangle=|u\rangle$, two diagonalizations (using TQLRAT) yield eigenvalues of J, denoted $\{\epsilon_\alpha\}$, and eigenvalues of the reduced Jacobi matrix in which b_1 is set to zero before diagonalization, denoted $\{\epsilon_\alpha^{(u)}\}$. From these two sets of eigenvalues, all residues $R_u(\alpha)$ [henceforth the diagonal residues $R_{AA}(\alpha)$ will be denoted $R_A(\alpha)$] are computed from Eq. (53). Priming the recursion method with the other starting vector $|0\rangle=|v\rangle$ then leads to two additional sets of eigenvalues $\{\epsilon_\alpha\}$ and $\{\epsilon_\alpha^{(v)}\}$. (Eigenvalues of the two full J matrices will be identical, for the $|u\rangle$ or $|v\rangle$ starting vectors.) The residues $R_v(\alpha)$ are then computed from an equation analogous to Eq. (53). The transition residues $R_{if}(\alpha)$ then follow very simply from Eq. (55).

A significant feature of the recursion method is that the number of chain links n needed for convergence is usually *much smaller* than N, the size of the original molecular basis. In effect, most of the physics of the $i\rightarrow f$ transition is concentrated in a relatively small subspace (dimension n) of the full Hilbert space. As recursion proceeds, each chain link generates a more distant environment of the transition of interest. As a result, the eigenvalues and largest residues which are most important for the $i\rightarrow f$ transition are generated quickly; refinement of these values along with the generation of small residues and their eigenvalues occurs as n increases. This feature will be demonstrated in the next section. The same effect was seen in earlier applications of the Lanczos method in solid-state physics[22] and in magnetic-resonance line-shape calculations.[26(c),26(d)]

As recursion proceeds, rounding errors in finite precision arithmetic lead to loss of significant figures which produces a gradual (after 30—50 steps) loss of global orthogonality (but not linear independence) in the recursion basis. Numerical experience has shown that this results in multiple copies of some eigenvalues, usually those on the edges of the range of eigenvalues. In addition, some "incorrect eigenvalues" (i.e., eigenvalues which are poor approximations to any real eigenvalues) are produced, which eventually settle onto actual eigenvalues as n increases. These spurious eigenvalues[20] must be removed from the eigenvalue lists before computing residues from Eq. (53). This is accomplished in a two-step procedure. First (for the recursion basis evolved from $|0\rangle=|u\rangle$), multiple copies of eigenvalues are deleted from both lists $\{\epsilon_\alpha\}$ and $\{\epsilon_\alpha^{(u)}\}$. That is, if $|\epsilon_\alpha-\epsilon_{\alpha+1}|<\sigma$, then $\epsilon_{\alpha+1}$ is deleted from the $\{\epsilon_\alpha\}$ list. The same procedure is followed for the list $\{\epsilon_\alpha^{(u)}\}$. For the model Hamiltonian in Sec. IV, $\sigma=10^{-5}$ was used. Next, the lists $\{\epsilon_\alpha\}$ and $\{\epsilon_\alpha^{(u)}\}$ are compared to see if there are any eigenvalues for which $|\epsilon_\alpha-\epsilon_\alpha(u)|<\sigma$. If so, *both* of these eigenvalues are deleted from their respective lists. The two sets of eigenvalues must interweave, $\epsilon_\alpha<\epsilon_\alpha^{(u)}<\epsilon_{\alpha+1}$, so that a near coincidence is regarded as an indication of spurious eigenvalues in *both* lists. This procedure has also been extensively employed by Cullum and Willoughby[20] in their use of the Lanczos method to generate eigenvalues of large matrices. The selective reorthogonalization method of Parlett and Scott[19] could be used to eliminate problems associated with spurious eigenvalues, but it is sufficient, and simpler, to merely follow the above procedure to contract the lists of eigenvalues at the end of the calculation.

Computations with the Lanczos recursion procedure are greatly aided if M is a sparse matrix. For the algebraic Hamiltonian in Sec. IV, this is the case; the fraction of nonzero elements is generally less than 5%. In this event, only the nonzero elements M_{ij} are computed and stored on disk. Batches of these elements (usually 20 000 at a time) are then read into fast storage in order to compute $M|n\rangle$ in Eq. (56). However, if M is relatively small and sparse, it is possible to store all of the nonzero elements in high-speed memory at one time. Another possibility is that if there is discernable symmetry in the pattern of off-diagonal elements (e.g., repeating blocks of nonzero elements in particular off-diagonal(s)), then a specialized multiplier for $M|n\rangle$ may be designed to greatly speed up the recursion process. Utilization of *structured sparsity* will be treated in more detail elsewhere.[33]

IV. NUMERICAL RESULTS: MULTIPHOTON EXCITATION IN A MODEL SYSTEM

A. Model Hamiltonian

In this section, the model Hamiltonian used for computations in Secs. IV B—IV E will be described. We assume that a monochromatic laser is coupled through the dipole operator to a Morse oscillator, which in turn is coupled to a "bath" of N_b harmonic oscillators. The field-free Hamiltonian is

$$H_m = Aa^\dagger a - B(a^\dagger a)^2 + \sum_{i=1}^{N_b} \hbar\omega_i b_i^\dagger b_i + \sum_{i=1}^{N_b} V_{\rm int}^{(i)}(a^\dagger b_i + a b_i^\dagger) , \quad (57)$$

where $\{a^\dagger, a\}$ and $\{b_i^\dagger, b_i\}$ are boson raising and lowering operators for the anharmonic oscillator (pump mode) and for one of the harmonic modes, respectively. The operators $\{a^\dagger, a\}$ for the Morse oscillator are discussed by Leasure.[7] In addition, A and B are related to D, the dissociation energy, and $\hbar\omega_a$, the zero-order frequency. Several additional remarks should be made about the terms in this Hamiltonian: (1) the N_b harmonic degrees of freedom are uncoupled from one another (the bath has been diagonalized); (2) the last term in this equation controls pump mode-bath energy exchange; $V_{\rm int}^{(i)}$ determines the strength of intramolecular VV coupling. This is a restricted quantum exchange[34] model in which $a^\dagger b_i$ allows feedback of energy (through single quantum exchange) from the bath mode back to the pump mode. A similar Hamiltonian has been used to model laser interaction with an adatom on a surface[35] and to study classical chaos in multiphoton excitation.[36]

The time-dependent coupling Hamiltonian is assumed to have the form

$$H_1(t) = \mu_1(a + a^\dagger)E^0\cos(\omega t) , \quad (58)$$

which allows nearest-neighbor $n \rightarrow n \pm 1$ coupling in the pump mode. Leasure[7] has shown how *any* dipole coupling operator for the Morse oscillator can be written as a series in the products $(a^\dagger)^l(a)^m$.

For the computations in this section, $N_b = 4$, so that there are altogether $N_b + 1 = 5$ "molecular" modes (of which only one is infrared active). If we then allow a maximum of p vibrational states in each mode, there will be a total of $N = p^5$ states in the molecular basis. In this study, $p = 3$, 4, or 5, so that the bases contained 243, 1024, or 3125 states, respectively. Parameters in this model Hamiltonian are listed in Table I. Note that the harmonic energy spacing for the pump mode is 1.0 energy unit (where one "energy unit" equals 1000 $\rm cm^{-1}$). The states cluster into bands, with one state in the lowest band, five states in band 2, etc.

The basis functions chosen to represent the quasienergy operator are products of harmonic oscillator functions,

$$|n_a\rangle\,|n_1\rangle\,|n_2\rangle\,|n_3\rangle\,|n_4\rangle ,$$

where $n_i = 0,1,2,\ldots$. Of course, these are eigenfunctions of part of the molecular Hamiltonian in Eq. (57), namely

$$Aa^\dagger a - B(a^\dagger a)^2 + \sum_{i=1}^{N_b} \hbar\omega_i b_i^\dagger b_i .$$

In this study, we will concentrate on transitions between these basis states which are induced by the combined effect of both the intramolecular, $ab_i^\dagger + a^\dagger b_i$, and the dipole coupling operator, $a + a^\dagger$. However, in realistic applications, it would be better to prediagonalize each quasidegenerate band of basis states, and then study laser-induced transitions between these approximate molecular eigenstates. Finally, in this study, we used the Magnus expansion for M in Eqs. (32)—(34), correct through *first order* in both types of coupling operators.

B. Comparison between diagonalization and recursion results

For relatively small basis sets, it is important to compare "exact" eigenvalues and residues from direct diagonalization of M with those from the recursion method. In this section, comparisons will be presented for $N = 243$, which arises when three basis functions are available in each of the five modes of the Hamiltonian in Eq. (57). First, for 150 recursion steps, Table II (for "weak" coupling, $V_{\rm int} = 0.01$, $V_{\rm rad} = 0.02$) compares the lowest 20 eigenvalues and residues for the initial recursion vectors $|i\rangle = |i-1,0,0,0,0\rangle$, for $i = 1$—3. The eigenvalues agree to better than 1% with their "exact" counterparts. The residues for $i = 1,2$ also agree well, although errors for $i = 3$ in the largest residues can be as large as 10%. Errors

TABLE I. Parameters for model Hamiltonian [Eq. (57)].

Symbol	Description	Value[a]
A	Pump mode harmonic frequency	1.0
B	Pump mode anharmonicity	0.02
$\omega_1,\omega_2,\omega_3,\omega_4$	Harmonic bath mode frequencies	0.97,0.99,1.01,1.03
$V_{\rm int}^{(i)}$	Intramolecular coupling strength[b]	0.01 (weak)
		0.03 (strong)
$V_{\rm rad} = \mu_1 E^0$	Radiative coupling strength	0.02 (weak)
		0.04 (strong)
ω	Laser frequency	1.0

[a] In units of 10^3 $\rm cm^{-1}$.
[b] $V_{\rm int}^{(i)}$ is the same for all modes, $i = 1, \ldots, 4$.

TABLE II. Comparisons of eigenvalues and residues, for different initial vectors, $N=243$. Diag. means diagonalization results. Recur. refers to the recursive scheme with 150 recursion steps. ($V_{\text{int}}=0.01, V_{\text{rad}}=0.02$; other parameters listed in Table I.)

$\|u\rangle=\|1\rangle$				$\|u\rangle=\|2\rangle$		$\|u\rangle=\|3\rangle$	
Diag.		Recur.		Diag.	Recur.	Diag.	Recur.
E_α	$R_{11}(\alpha)$	E_α	$R_{11}(\alpha)$	$R_{22}(\alpha)$	$R_{22}(\alpha)$	$R_{33}(\alpha)$	$R_{33}(\alpha)$
−0.000 41	0.999 58	−0.000 41	0.999 58	0.000 42	0.000 42	0.000 00	0.000 00
0.960 96	0.000 17	0.960 92	0.000 17	0.394 97	0.396 98	0.000 36	0.000 40
0.977 92	0.000 13	0.977 88	0.000 13	0.301 36	0.300 83	0.000 27	0.000 31
0.994 49	0.000 07	0.994 48	0.000 07	0.170 99	0.170 11	0.000 16	0.000 17
1.012 68	0.000 03	1.012 67	0.000 03	0.082 69	0.082 25	0.000 08	0.000 09
1.031 87	0.000 02	1.031 87	0.000 02	0.048 68	0.048 44	0.000 04	0.000 05
1.905 87	0.000 00	1.912 39	0.000 00	0.000 65	0.000 80	0.710 40	0.784 66
1.930 84		1.933 19		0.000 10	0.000 10	0.111 35	0.094 72
1.950 49		1.948 15		0.000 06	0.000 06	0.067 10	0.058 05
1.956 09		1.955 92		0.000 00	0.000 00	0.000 10	0.000 68
1.969 56		1.969 53		0.000 04	0.000 03	0.044 93	0.029 41
1.973 65		1.984 98				0.001 19	0.009 11
1.988 13		1.990 09		0.000 02	0.000 00	0.024 75	0.006 61
1.990 25		1.993 13				0.004 95	0.001 17
1.992 76		2.006 84				0.003 58	0.007 37
2.006 84		2.010 01		0.000 01	0.000 00	0.012 15	0.001 49
2.009 69		2.022 90				0.005 46	0.001 17
2.025 54		2.026 45				0.004 79	0.002 46
2.026 46		2.044 77				0.003 69	0.001 72
2.044 75		2.061 93				0.003 48	0.000 34

in the residues are due to small shifts in the eigenvalues of both M and the reduced matrix $M^{(u)}$ from their exact values.

Table III present similar comparisons for the "strong" coupling case ($V_{\text{int}}=0.03, V_{\text{rad}}=0.04$) for the $1\rightarrow 3$ transition. Errors in the largest residues are usually below 5%. Fortunately, there is a partial cancellation of errors in the individual residues when R_{if} is computed from Eq. (55).

The most significant comparison between the two methods is for the time evolution of individual transition probabilities. From the eigenvalues and residues, survival probabilities, $\langle 1 \mid U(t \mid 0) \mid 1\rangle^2$, were compared (not shown here) for both early ($0 \leq t \leq 0.20$ ps) and late ($1.00 \leq t \leq 1.0002$ ns) times. In spite of the eigenvalue and

TABLE III. Comparison of residues for $1\rightarrow 3$ transition, $N=243$. 100 recursion steps were used.

α	Diagonalization		Recursion	
	E_α	$R_{13}(\alpha)$	E_α	$R_{13}(\alpha)$
1	−0.001 639	0.001 208 46	−0.001 639	0.001 281 52
2	0.924 353	−0.001 366 69	0.924 143	−0.001 445 26
3	0.976 096	−0.000 105 86	0.976 078	−0.000 111 91
4	0.997 410	−0.000 111 98	0.997 390	−0.000 118 81
5	1.018 747	−0.000 115 61	1.018 726	−0.000 123 15
6	1.055 068	−0.000 761 76	1.054 916	−0.000 809 83
7	1.838 724	0.000 553 19	1.843 343	0.000 572 07
8	1.900 306	0.000 073 52	1.902 224	0.000 084 46
9	1.921 467	0.000 077 26	1.922 662	0.000 089 59
10	1.942 607	0.000 085 57	1.943 309	0.000 101 15
11	1.953 757	0.000 003 04	1.953 135	0.000 003 76
12	1.969 962	0.000 307 01	1.969 125	0.000 325 79
13	1.975 283	0.000 004 33	1.975 229	0.000 003 66
14	1.996 353	0.000 002 11	1.996 174	0.000 002 33
15	1.996 469	0.000 000 01	a	
16	2.017 675	0.000 003 01	2.017 573	0.000 003 42
17	2.031 979	0.000 021 05	2.030 892	0.000 021 51
18	2.039 071	0.000 001 49	2.039 069	0.000 001 99
19	2.053 209	0.000 023 05	2.051 798	0.000 022 98
20	2.074 484	0.000 024 35	2.072 412	0.000 023 81
21	2.108 569	0.000 074 38	2.105 445	0.000 070 93
22	2.788 861	0.000 000 01	2.793 659	0.000 000 01

[a]An eigenvalue close to this exact value was not returned in the recursion procedure.

TABLE IV. Comparisons of time evolution, $N=243$. (All probabilities $\times 10^2$.)

t (ps)	$P_{12}(t)$ Diagonalization	$P_{12}(t)$ Recursion[a]	$P_{13}(t)$ Diagonalization	$P_{13}(t)$ Recursion[a]
0.01	0.4202	0.4202	0.9095	0.9095
0.02	0.6050	0.6050	2.0627	2.0625
0.03	0.0897	0.0898	0.0687	0.0686
0.04	0.1575	0.1575	0.0929	0.0930
0.05	0.5622	0.5622	1.6249	1.6245
0.06	0.2677	0.2678	0.5382	0.5382
0.07	0.0216	0.0216	0.0275	0.0275
0.08	0.3369	0.3369	0.4399	0.4402
0.09	0.3566	0.3566	0.8289	0.8292
0.10	0.0798	0.0798	0.0135	0.0135
1000.00	0.4599	0.4599	0.6181	0.8739
1000.01	0.2477	0.2477	0.3934	0.5254
1000.02	0.1812	0.1812	0.0202	0.0802
1000.03	0.4173	0.4173	0.4573	0.6752
1000.04	0.4886	0.4887	0.8799	0.9838
1000.05	0.0420	0.0420	0.2196	0.2234
1000.06	0.2195	0.2195	0.4002	0.5837
1000.07	0.5856	0.5856	0.8395	0.9207
1000.08	0.2131	0.2131	0.6477	0.5055
1000.09	0.0437	0.0437	0.2213	0.2437
1000.10	0.4576	0.4574	1.0029	1.0080

[a]100 recursion steps were used.

residue errors, the survival probabilities are usually accurate to about 1 part in 10^5. In Table IV, probabilities for the $1\rightarrow 2$ and $1\rightarrow 3$ transitions are shown for both early ($0\leq t\leq 0.1$ ps) and late ($1.0000\leq t\leq 1.0001$ ns) times. For the $1\rightarrow 2$ transition, errors as large as 1 part in 4000 arise, while for the $1\rightarrow 3$ transition, the short-time results are again as accurate, but the long-time results show larger errors (the *absolute* error is about 10^{-6}, for probabilities the order of 10^{-5}). For both of these transitions, only 100 recursion steps were used to generate the eigenvalues and residues; the errors may be made as small as desired by increasing n, the number of chain links under consideration. That is, those residues and eigenvalues are accurately generated by the same recursion procedure (from $|u\rangle$ and $|v\rangle$) which are *needed* for the computation of $\langle f|U(t|0)|i\rangle$; small residues and their associated eigenvalues are computed relatively late in the recursion scheme.

C. Residue spectra

In order to illustrate some characteristics of residue spectra, Fig. 1 shows $R_u(\alpha)$, $R_v(\alpha)$, and $R_{if}(\alpha)$ for the $i=|2,0,0,0,0,0\rangle\rightarrow f=|3,0,0,0,0,0,\rangle$ transition. The residues are plotted as horizontal "sticks" at the appropriate eigenvalue E_α. The residues cluster around the energies of the zero-order states. Although the diagonal residues $R_u(\alpha)$ and $R_v(\alpha)$ are always positive numbers, the transition residue $R_{if}(\alpha)$ may assume positive and negative values.

Figure 2 illustrates how specification of $|i\rangle$ and $|f\rangle$ *preselects* those regions of the eigenvalue spectrum which will receive numerical emphasis. For $N=3125$, residues are plotted as vertical sticks, at the position of the associated eigenvalue, for the overtone sequence of initial recursion vectors $2^{-1/2}(|1\rangle+|f\rangle)$, with $f=2,\ldots,5$. In each case, there is a large residue (~ 0.5) near the ground-state energy $E=0$, and a bundle of residues near the energy of the "final" zero-order state ($E=1,2,3,4$, respectively). Most eigenvalues associated with small residues (<0.001) are not produced when $n\ll N$, as discussed in the next section. In this sense, the RRGM *automatically* concen-

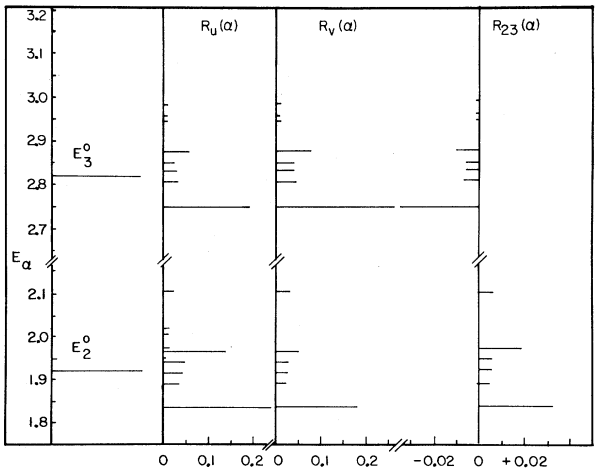

FIG. 1. Residue spectra for the $2\rightarrow 3$ transition, where state 2 is $|2,0,0,0,0,0,\rangle$ and state 3 is $|3,0,0,0,0,0,\rangle$. The left column shows the energies of the zero-order anharmonic states, computed from the Hamiltonian $A(a^\dagger a)-B(a^\dagger a)^2$. The middle two columns show residue spectra for the starting recursion vectors $|u\rangle$ and $|v\rangle$; $R_{23}(\alpha)=\frac{1}{2}[R_u(\alpha)-R_v(\alpha)]$.

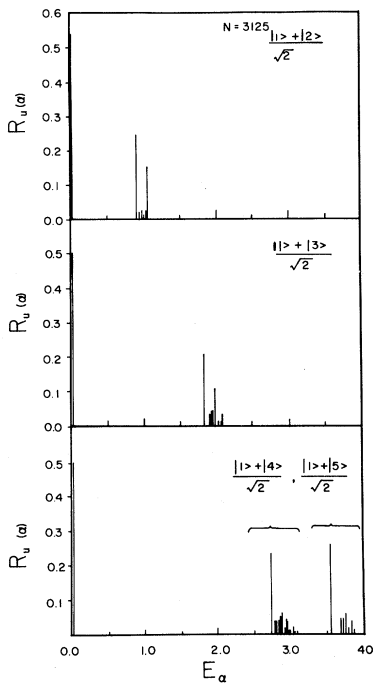

FIG. 2. Residue spectra, for four overtone transition vectors. The largest residues concentrate around the energies of the zero-order states. The basis size is 3125, and the strong coupling parameters from Table I were used.

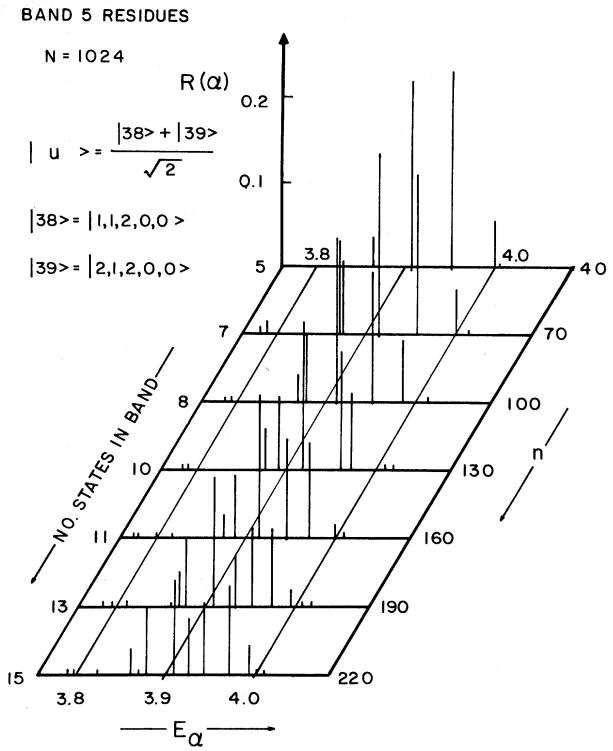

FIG. 3. Residue spectrum near $E=4$ for the initial recursion vector associated with the transition from state 38 to state 39 in the $N=1024$ system. The right axis gives the number of recursion steps (n), while the number of predicted states in this band is shown along the left axis.

trates its numerical effort just where it is needed, to produce large residues and their associated eigenvalues.

D. Dependence upon the number of recursion steps

For a specified initial recursion vector, say $|u\rangle$, the preceding analysis showed that eigenvalues and residues important for one particular transition are accurately generated. As n, the number of recursion steps increases; these "important" eigenvalues and eigenvectors converge to their final values, usually for $n \ll N$. For example, Fig. 3 shows residues in the band near $E=4$ for the transition vector $|u\rangle = 2^{-1/2}(|38\rangle + |39\rangle)$, for a system with $N=4^5=1024$ basis vectors, where $|38\rangle = |1,1,2,0,0\rangle$ and $|39\rangle = |2,1,2,0,0\rangle$. (The energy of unperturbed state number 38 is 3.93.) As n increases from 40 to 220, the number of eigenvalues predicted in this band increases from 5 to 15. *Eigenvalues corresponding to the largest residues are predicted first,* with refinement of these values occurring as n increases. Additional smaller residues are also generated as n increases. The eigenvalues and residues are essentially converged by the time $n=220$. Eigenvalues (and residues) *not* near the energies of these two unperturbed states are not among the first ones generated, at least for $n \ll N$. Of course, "how different" the initial and final states are determines the value of n required for convergence. Some typical values for pump mode transitions, with $|i\rangle = |1\rangle$ are $f=1, n=50$; $f=i+1, n=100$; $f=i+2, n=200$; $f=i+3, n=500$; $f=i+4, n=1000$. Very weak ($P_{if} \sim 10^{-6}$) overtone transitions required relatively large values of n (near $N/2$) for convergence. Otherwise, values of n around $N^{1/2}$ are sufficient for convergence. Rapid convergence of the local density of states with respect to the number of recursion steps in solid-state problems was noted previously.[22]

For a fixed basis size N, the number of chain links in the recursion controls the accuracy of the time-dependent transition probabilities. For example, Table V shows how

TABLE V. Convergence of the time-dependent transition probability $P_{13}(t)$ with respect to the number of iteration steps, $N=3125$. Entries are $10^4 P_{13}(t)$.

t (ps)	$n=75$	$N=100$	$n=150$
0.05	0.1677	0.1610	0.1611
0.15	0.0091	0.0057	0.0057
0.25	0.0030	0.0029	0.0029
0.35	0.0288	0.0254	0.0255
0.45	0.0841	0.0886	0.0886
0.55	0.0289	0.0387	0.0387
0.65	0.0043	0.0038	0.0038
1000.40	0.0968	0.0508	0.0510
1000.10	0.0534	0.0431	0.0429
1000.20	0.0013	0.0077	0.0078
1000.30	0.1024	0.1503	0.1516
1000.40	0.0642	0.0508	0.0503
1000.50	0.0138	0.0311	0.0305
1000.60	0.0251	0.0345	0.0348
1000.70	0.0615	0.0249	0.0245

TABLE VI. Basis size dependence of eigenvalues and residues (only values greater than 10^{-5} are listed here) for the initial recursion vector $|u\rangle = 2^{-1/2}[|2\rangle + |3\rangle]$.

	$N=243$[a]		$N=1024$[b]		$N=3125$[c]	
α	E_α	$R(\alpha)$	E_α	$R(\alpha)$	E_α	$R(\alpha)$
1	−0.001 64	0.500 44	−0.001 64	0.500 44	−0.001 64	0.500 44
2	0.924 14	0.000 11	0.924 14	0.000 11	0.924 14	0.000 11
3	1.054 91	0.000 12	1.054 91	0.000 12	1.054 91	0.000 12
4	1.843 34	0.198 51	1.840 92	0.209 11	1.840 91	0.209 14
5	1.902 22	0.031 22	1.901 87	0.031 88	1.901 87	0.031 89
6	1.922 66	0.033 81	1.922 23	0.034 15	1.922 29	0.034 15
7	1.943 31	0.038 98	1.942 89	0.039 44	1.942 89	0.039 44
8	1.953 13	0.001 46	1.953 11	0.001 48	1.953 12	0.001 48
9	1.969 12	0.128 82	1.967 85	0.118 29	1.967 85	0.118 25
10	1.975 22	0.001 45	1.975 21	0.000 92	1.975 21	0.000 90
11	1.996 09	0.000 63	1.996 07	0.000 52	1.996 08	0.000 56
12	1.996 34	0.000 32	1.996 30	0.000 31	1.996 34	0.000 27
13	2.017 57	0.001 43	2.017 56	0.001 32	2.017 56	0.001 32
14	2.030 89	0.009 09	2.030 80	0.008 48	2.030 80	0.008 48
15	2.039 07	0.000 85	2.039 06	0.000 79	2.039 06	0.000 79
16	2.051 80	0.009 92	2.051 71	0.009 31	2.051 71	0.009 31
17	2.072 41	0.010 49	2.072 31	0.009 89	2.072 32	0.009 90
18	2.105 44	0.032 28	2.105 18	0.030 37	2.105 17	0.030 36
19	2.793 66	0.000 01	2.734 10	0.001 42	2.731 19	0.001 51
20			2.812 14	0.000 23	2.811 56	0.000 24
21			2.833 75	0.000 23	2.833 20	0.000 22
22			2.854 76	0.000 24	2.854 17	0.000 23
23			2.876 43	0.000 40	2.875 21	0.000 32
Sum of residues		0.999 99		0.999 51		0.999 54

[a]150 recursion steps were used.
[b]150 recursion steps were used.
[c]250 recursion steps were used.

$P_{13}(t)$ varies with n, for two time intervals. In this case, convergence is reached around $n=100$, although the values for $n=75$ are qualitatively correct.

E. Basis size dependence

To predict a particular transition in a multistate system, it is not always necessary to include a very large number of basis states. Figure 4 shows the $1\rightarrow 2$ transition probability over the time interval $0<t<0.140$ ps for two different bases. Except when the transition probability falls below $\frac{1}{100}$ of the maximum value, even the $N=243$ basis adequately models this transition. This point is illustrated further in Table VI, which lists eigenvalues and residues for the $|u\rangle = 2^{-1/2}(|1\rangle + |3\rangle)$ initial recursion vector. In this case, most of the eigenvalues are accurate to 0.1% (except for $\alpha=19$, for the smallest basis). Also, there is little difference between the residues for the $N=243$ and 3125 state calculations.

V. CONCLUSION

In this study, we have seen that combining "discrete" Floquet theory with the RRGM allows the treatment of molecules interacting with intense driving fields with a much larger number of coupled states than are amenable using any other method. In fact, studies are being conducted of the model system in Sec. IV with ~40 000 states.[33] As far as the RRGM itself is concerned, we would like to emphasize that it does not depend upon Floquet theory (e.g., other time-independent Hamiltonians can be used for the laser-molecule problem, including those provided by the rotating wave and rotating frame[37] approximations) or the laser-molecule context, but is de-

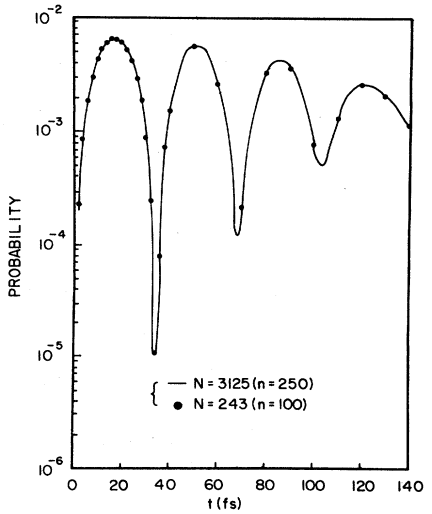

FIG. 4. Time dependence of the $1\rightarrow 2$ transition probability for two different basis sets.

vised for the evaluation of any transition amplitude $\langle f \mid \exp(-iMt/\hbar) \mid i \rangle$ involving a time-independent generator M to advance the system. Therefore, the RRGM is likely to be useful for a variety of other problems (e.g., the evaluation of time-dependent correlation functions in statistical mechanics,[38] classical statistical mechanics, scattering theory, etc.).

ACKNOWLEDGMENTS

For helpful discussions, we thank Xavier Chapuisat, Kent Milfeld, and José Castillo. This work was supported in part by the Robert A. Welch Foundation of Houston, Texas and the National Science Foundation.

*Permanent address: Laboratoire de Chimie Quantique, Bâtiment Lavoisier, Université Catholique de Louvain, B-1348 Louvain-la-Neuve, Belgium and Laboratoire de Chimie Théorique, (Equipe de Recherche No. 549 associée au Centre National de la Recherche Scientifique), Bâtiment 490, Faculté des Sciences, Université de Paris—Sud, F-91405 Orsay Cedex, France.

[1]C. D. Cantrell, S. M. Freund, and J. L. Lyman, in *The Laser Handbook,* edited by M. L. Stitch (North-Holland, New York, 1979), Vol. 3, p. 485; C. D. Cantrell, V. S. Letokhov, and A.A. Makarov, in *Topics in Current Physics,* edited by M. S. Feld and V. S. Letokhov, (Springer, Heidelberg, 1980), Vol. 21, p. 165; V. S. Letokhov, Phys. Today 33, 34 (1980); H. G. Galbraith and J. R. Ackerhalt, in *Laser Induced Chemical Processes,* edited by J. I. Steinfeld (Plenum, New York, 1981), p. 1; M. Quack, in *Dynamics of the Excited State,* edited by K. P. Lawley (Wiley, New York, 1982), p. 385; T. F. George, J. Phys. Chem. 86, 10 (1982); D. S. King, in *Dynamics of the Excited State,* p. 105.

[2]J. H. Shirley, Phys. Rev. 138, 979 (1965).

[3]D. R. Dion and J. O. Hirschfelder, Adv. Chem. Phys. 35, 265 (1976); P. K. Aravind and J. O. Hirschfelder (unpublished).

[4]J. V. Moloney and W. J. Meath, Mol. Phys. 31, 1537 (1976); 35, 1163 (1978); G. F. Thomas, J. Chem. Phys. 79, 4912 (1983).

[5]S. I. Chu, J. V. Tietz, and K. Datta, J. Chem. Phys. 77, 2968 (1982); S. I. Chu, Chem. Phys. Lett. 58, 462 (1978); 64, 178 (1979); 70, 205, (1980); S. I. Chu, J. Chem. Phys. 75, 2215 (1981); T. S. Ho, S. I. Chu, and J. V. Tietz, Chem. Phys. Lett. 96, 464 (1983); S. I. Chu, C. Laughlin, and K. V. Datta, *ibid.* 98, 476 (1983).

[6]D. C. Clary, Mol. Phys. 46, 1099 (1982); D. C. Clary and J. P. Henshaw, J. Phys. Chem. (in press); D. C. Clary, *ibid.* 87, 735 (1983).

[7]S. Leasure, Chem. Phys. 67, 83 (1982).

[8](a) S. C. Leasure and R. E. Wyatt, Opt. Eng. 19, 46 (1980); (b) S. C. Leasure, K. F. Milfeld, and R. E. Wyatt, J. Chem. Phys. 74, 6197 (1981); (c) K. F. Milfeld and R. E. Wyatt, Phys. Rev. A 27, 72 (1983); (d) M. J. Davis, R. E. Wyatt, and C. Leforestier, in *Intramolecular Dynamics,* edited by J. Jortner and B. Pullman (Reidel, Dordrecht, 1982), p. 403; (e) C. Leforestier and R. E. Wyatt, J. Chem. Phys. 78, 2234 (1983).

[9]H. Sambe, Phys. Rev. A 7, 2203 (1973).

[10]S. R. Barone, M. A. Narcowich, and F. J. Narcowich, Phys. Rev. A 15, 1109 (1977).

[11]F. Gesztesy and H. Mitter, J. Phys. A 14, L79 (1981).

[12]W. R. Salzman, Phys. Rev. A 10, 461 (1974).

[13]P. Pechukas and J. C. Light, J. Chem. Phys. 44, 3897 (1965); D. W. Robinson, Helv. Phys. Acta 36, 140 (1963).

[14]A. Nauts and R. E. Wyatt, Phys. Rev. Lett. 51, 2238 (1983).

[15]C. Lanczos, J. Res. Natl. Bur. Stand. 45, 255 (1950).

[16]B. N. Parlett, *The Symmetric Eigenvalue Problem* (Prentice-Hall, Englewood Cliffs, N.J., 1980), Chap. 13.

[17]*Numerical Algorithms in Chemistry: Algebraic Methods,* edited by C. Moler and I. Shavitt (NRCC, Lawrence Berkeley Laboratory, 1978).

[18]C. C. Paige, J. Inst. Math. Appl. 10, 373 (1972); 18, 341 (1976).

[19]B. N. Parlett and D. S. Scott, Math. Comp. 33, 217 (1979).

[20]J. Cullum and R. A. Willoughby, J. Comp. Phys. 44, 329 (1981).

[21]R. Haydock, Comp. Phys. Commun. 20, 11 (1980).

[22]R. Haydock, in *Solid State Physics,* edited by H. Ehrenreich, F. Seitz, and D. Turnbull, (Academic, New York, 1980), Vol. 35, p. 215.

[23]R. Haydock, in *Excitations in Disordered Systems,* (Plenum, New York, 1981), p. 29.

[24]S. Muramatsu and N. Sakamato, J. Phys. Soc. Jpn. 46, 1273 (1979); S. N. Evangelou, M. C. M. O'Brien, and R. S. Perkins, J. Phys. C 13, 4175 (1980); J. R. Fletcher and D. R. Pooler, J. Phys. C 15, 2695 (1982); E. Haller, H. Köppel, L. S. Cederbaum, W. von Niessen, and G. Bieri, J. Chem. Phys. 78, 1359 (1983).

[25]E. Haller, H. Köppel, and L. S. Cederbaum (unpublished).

[26](a) A. Baram, Mol. Phys. 45, 309 (1982); (b) S. Alexander, A. Baram, and Z. Luz, J. Chem. Phys. 61, 992 (1974); (c) G. Moro and J. H. Freed, J. Phys. Chem. 84, 2837 (1980); (d) J. Chem. Phys. 74, 3757 (1981).

[27]P. W. Langhoff, in *Methods in Computational Molecular Physics* edited by G. H. Diercksen and S. Wilson (Reidel, Dordrecht, 1983), p. 299; M. R. Hermann and P. W. Langhoff, Int. J. Quantum Chem. 23, 135 (1983).

[28](a) A. Messiah, *Quantum Mechanics* (Wiley, New York, 1950) Vol. II, Chap. 15, Secs. 5 and 19. (b) See Ref. 28(a), Chap. 15, Sec. 20.

[29]M. L. Goldberger and K. M. Watson, *Collision Theory* (Wiley, New York, 1964), Chap. 8; L. Mower, Phys. Rev. 142, 799 (1966).

[30]*Solid State Physics,* Ref. 22, pp. 250 and 251.

[31]Z. Nehari, *Introduction to Complex Analysis* (Allyn and Bacon, Boston, 1951), p. 124.

[32]*Solid State Physics,* Ref. 22, pp. 222—231.

[33]J. E. Castillo and R. E. Wyatt (unpublished).

[34]J. Stone, M. F. Goodman, and E. Thiele, Chem. Phys. Lett. 71, 171 (1980); K. G. Kay, J. Stone, E. Thiele, and M. F. Goodman, *ibid.* 82, 539 (1981); J. Stone, E. Thiele, and M. F. Goodman, J. Chem. Phys. 75, 1712 (1981).

[35]M. S. Slutsky and T. F. George, Chem. Phys. Lett. 57, 474 (1978).

[36]J. R. Ackerhalt, H. W. Galbraith, and P. W. Milonni, Phys. Rev. Lett. 51, 1259 (1983).

[37]K. B. Whaley and J. C. Light, Phys. Rev. A 29, 1188 (1984).

[38]R. A. Friesner and R. E. Wyatt (unpublished).